

# Ring-Current Models from the Differential Biot-Savart Law

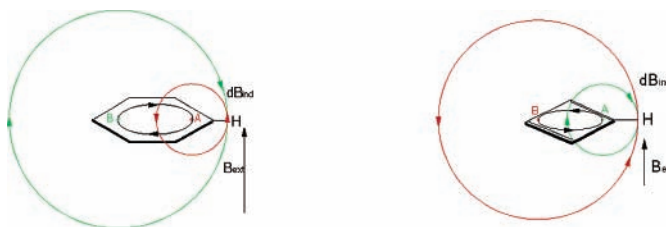
S. Pelloni, A. Ligabue, and P. Lazzeretti\*

Dipartimento di Chimica, Università degli Studi di Modena e Reggio Emilia,  
via G. Campi 183, 41100 Modena, Italy

lazzeret@unimo.it

Received August 20, 2004

## ABSTRACT



The differential Biot-Savart law provides simple models for the  $\pi$  ring currents induced in diatropic and paratropic planar conjugated molecules by a perpendicular magnetic field. The model predictions are confirmed by ab initio maps of nuclear magnetic shielding density. The effects on the protons and on the ring carbon atoms from the closest and furthest segments of the current loop are easily interpreted.

The integral Biot-Savart (IBS) law<sup>1</sup> gives the magnetic field  $\mathbf{B}_{\text{ind}}(\mathbf{R}_J)$  induced at a point  $\mathbf{R}_J$ , the position of nucleus  $J$ , by the current density  $\mathbf{J}^{\mathbf{B}}(\mathbf{r})$  generated by an external, static, and spatially uniform magnetic field  $\mathbf{B}$ . The effective field at  $\mathbf{R}_J$  is  $\mathbf{B} + \mathbf{B}_{\text{ind}}(\mathbf{R}_J)$ . The nuclear magnetic shielding is described by the tensor  $\sigma(\mathbf{R}_J)$

$$\sigma_{\alpha\delta}(\mathbf{R}_J) \equiv \sigma_{\alpha\delta}^J = -\frac{1}{c} \epsilon_{\alpha\beta\gamma} \int d^3r \frac{r_\beta - R_{J\beta}}{|\mathbf{r} - \mathbf{R}_J|^3} \mathcal{J}_\gamma^{\mathbf{B}_\delta}(\mathbf{r}) \quad (1)$$

where the Einstein convention for summing over repeated Greek indices is in force;  $\epsilon_{\alpha\beta\gamma}$  is the Levi-Civita tensor, and  $\mathcal{J}_\gamma^{\mathbf{B}_\delta} = \partial J_\gamma^{\mathbf{B}_\delta} / \partial B_\delta$  is the current density tensor. The integrand in eq 1 is a function of position in real space, defining a shielding density,<sup>2,3</sup> whose components can be plotted over a plane specified by fixing one coordinate. The representation of  $\mathbf{J}^{\mathbf{B}}$  and the corresponding shielding density maps provide complementary pieces of information useful for analyzing the regions where shielding/deshielding occur and for developing interpretative models.<sup>4,5</sup>

For instance, despite the fact that a few authors regard this model as wrong,<sup>7</sup> the IBS law is used extensively to explain the anomalous deshielding of arene proton chemical shifts via the ring-current model (RCM).<sup>6,8–16</sup> The RCM predicts that an external field  $(0, 0, B_z)$  perpendicular to the molecular  $xy$  plane of benzene induces  $\pi$ -electron ring currents, which can be probed by the magnetic dipole  $\mu_{\text{H}}$  of the H nucleus via the electron-coupled interaction energy  $\mu_{\text{H}\alpha} \sigma_{\alpha\beta}^{\text{H}} B_\beta$ .

The ring currents reduce the magnitude of the out-of-plane component  $\sigma_{zz}^{\text{H}}$ . One-third of this effect is observable in nuclear magnetic resonance (NMR) spectra of molecules in

(1) Jackson, J. D. *Classical Electrodynamics*, 3rd ed.; John Wiley & Sons: New York, 1999.

(2) Jameson, C. J.; Buckingham, A. D. *J. Phys. Chem.* **1979**, *83*, 3366.

(3) Jameson, C. J.; Buckingham, A. D. *J. Chem. Phys.* **1980**, *73*, 5684.

(4) Keith, T. A.; Bader, R. F. W. *Can. J. Chem.* **1996**, *74*, 185.

(5) Ferraro, M. B.; Lazzeretti, P.; Viglione, R. G.; Zanasi, R. *Chem. Phys. Lett.* **2004**, *390*, 268.

(6) Soncini, A.; Fowler, P. W.; Lazzeretti, P.; Zanasi, R. Submitted to CPL. The notion, based on the DBS law, that H and C shielding-density maps contain signatures of global ring currents, was already set out in this reference for three typical aromatic, nonaromatic and antiaromatic systems.

(7) Wannere, C. S.; Schleyer, P. v. R. *Org. Lett.* **2003**, *5*, 605.

(8) Salem, L. *The Molecular Orbital Theory of Conjugated Systems*; W. A. Benjamin, Inc.: New York, 1966.

(9) Mallion, R. B. *Mol. Phys.* **1973**, *25*, 1415.

(10) Haddon, R. C. *Tetrahedron* **1972**, *28*, 3613.

(11) Haddon, R. C. *Tetrahedron* **1972**, *28*, 3635.

(12) Fleischer, U.; Kutzelnigg, W.; Lazzeretti, P.; Mühlenkamp, V. *J. Am. Chem. Soc.* **1994**, *116*, 5298.

(13) Lazzeretti, P. Ring currents. In *Progress in Nuclear Magnetic Resonance Spectroscopy*; Elsevier: New York, 2000; Vol. 36, p 1–88.

(14) von Ragué Schleyer, P. *Chem. Rev.* **2001**, *101*, 1115.

(15) Gomes, J. A. N. F.; Mallion, R. B. *Chem. Rev.* **2001**, *101*, 1349.

(16) Havenith, R. W. A.; Jenneskens, L. W.; Fowler, P. W. *Chem. Phys. Lett.* **2003**, *367*, 468.

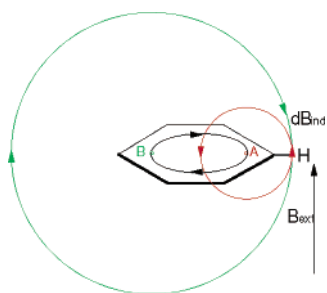


**Figure 1.** Ring-current model for benzene from the DBS law. The external magnetic field  $\mathbf{B}_{\text{ext}}$  perpendicular to the molecular  $xy$  plane induces a diamagnetic (clockwise) current density in the  $\pi$  electrons. The  $\pi$  current through point A (B) generates an elemental magnetic field  $d\mathbf{B}_{\text{ind}}$ , red (green) line, reinforcing (diminishing)  $\mathbf{B}_{\text{ext}}$  at the site of H proton, and causes deshielding (shielding) by lowering (enhancing) the out-of-plane component  $\sigma_{zz}^{\text{H}}$ .

disordered phase as a low-field chemical shift of the trace  $1/3\sigma_{\alpha\alpha}^{\text{H}}$  with respect to a reference compound.<sup>8</sup>

However, in some situations, the IBS law is not the most useful form for magnetostatic, and the differential relationship (DBS) is more convenient.<sup>1</sup> In the case of a current generated by an external  $\mathbf{B}$ , the current element  $I d\mathbf{l} = \mathbf{J}^{\text{B}} d^3r$ , and the DBS equation is cast in the form

$$d\mathbf{B}_{\text{ind}}(\mathbf{r}) = \frac{1}{c} \mathbf{J}^{\text{B}} \times \frac{\mathbf{r}}{|\mathbf{r}|^3} d^3r = -\Sigma(\mathbf{r}) \cdot \mathbf{B} d^3r \quad (2)$$

with

$$\Sigma_{\alpha\delta}(\mathbf{r}) = \frac{1}{c} \epsilon_{\alpha\beta\gamma} \frac{r_{\beta}}{|\mathbf{r}|^3} \mathcal{J}_{\gamma}^{\text{B}\delta} \quad (3)$$

the shielding density<sup>2,3</sup> at  $P$ . The simple law (2) is sufficient to evaluate the sign of the elemental flux density  $d\mathbf{B}_{\text{ind}}$  and of the components of  $\Sigma_{\alpha\delta}$  at any  $P$ .

The interpretative power of the DBS-based model in Figure 1 for elemental shielding at benzenic protons is understood by simple considerations. According to eq 2, the current element in the proximity of the point A reinforces the external field at H, decreases the shielding density component  $\Sigma_{zz}^{\text{H}}$  in the region of the proton, and determines an elemental downfield (paramagnetic) shift at the H nucleus. The out-of-plane component  $\sigma_{zz}^{\text{H}}$  is reduced. On the other hand, the current element in the vicinity of B decreases the field at the probe, increases  $\Sigma_{zz}^{\text{H}}$  in its vicinity, and has an opposite elemental *shielding* effect on the proton, i.e.,  $\sigma_{zz}^{\text{H}}$  increases.

If it is assumed that the modulus of the  $\pi$ -ring current is the same all over the circuit, the BS law (2) tells us that A and B are local extremum points of the elemental flux density  $d\mathbf{B}_{\text{ind},z}$  at the proton as a function of the position of  $\mathbf{J}^{\text{B}}$ , since  $d\mathbf{B}_{\text{ind}}$  depends on the sine of the angle between the  $\mathbf{J}^{\text{B}}$  and  $\mathbf{r}$  vectors.

As the magnetic flux density at H changes sign on passing from the region of the para to that of the ipso carbon, it must vanish somewhere in between. From eq 2 it is seen

that the vector product vanishes if  $\mathbf{J}^{\text{B}}$  and  $\mathbf{r}$  are parallel or antiparallel. In the model of Figure 1 there are a couple of such points, on different sides with respect to the A–B direction, approximately in the zone of ortho carbons.

Corresponding considerations are easily made for  $\Sigma_{zz}^{\text{H}}$  allowing for the second identity of (2), e.g., the points A and B are also extremum points of the proton shielding density function. Deshielding at the site of the probe H is overwhelming, as the contribution to the proton shielding density from  $\mathbf{J}^{\text{B}}$  at point B is comparatively much weaker than that at the point A, due to its  $r^{-2}$  dependence.<sup>17</sup>

Plots of the shielding density

$$\Sigma_{zz}^{\text{H}}(\mathbf{r}) = -\frac{1}{c} \epsilon_{z\beta\gamma} \frac{r_{\beta} - R_{\text{HB}}}{|\mathbf{r} - \mathbf{R}_{\text{H}}|^3} \mathcal{J}_{\gamma}^{\text{B}_z}(\mathbf{r}) \quad (4)$$

obtained by accurate calculations of the quantum mechanical current density confirm the reliability of the RCM in Figure 1.<sup>5</sup> The maps of  $\Sigma_{zz}^{\text{H}}$  are characterized by (i) a deep deshielding spike localized about the ipso carbon (ii) a shielding crest in the region of the meta and para carbons (iii) a nodal region in the proximity of the ortho carbon atoms.<sup>4,5</sup>

The model of Figure 1 suggests that the distant  $\pi$  ring currents also bias the out-of-plane component of C shielding in benzene. The local effect on a C nucleus, carrying the magnetic dipole  $\mu_{\text{C}}$ , exerted by the  $\pi$  diamagnetic ring currents in which it is embedded, should approximately vanish, since, according to the BS law, the induced magnetic field changes sign on crossing the current loop. However, shielding is expected from the current over the carbon nucleus on the opposite side. The maps of ab initio  $\Sigma_{zz}^{\text{C}}$  confirm this prediction, vide infra the discussion of Figure 5.

One can ask if a simple model based on the DBS law like that of Figure 1 can be devised to investigate the paratropism of antiaromatic systems. The cyclobutadiene molecule has been examined in this study. A non contracted (13s10p5d2f/8s4p1d) basis set,<sup>18</sup> containing 476 Gaussians, was adopted to evaluate magnetizability, nuclear shielding of H and C nuclei, and function (4) by the coupled Hartree–Fock (CHF) approximation,<sup>19</sup> within the procedure of continuous transformation of the origin of the current density-diamagnetic zero (CTOCD-DZ) and paramagnetic zero (PZ).<sup>13</sup> The parameters  $r_{\text{C}=\text{C}} = 1.331693 \text{ \AA}$ ,  $r_{\text{C}-\text{C}} = 1.578485 \text{ \AA}$ ,  $r_{\text{C}-\text{H}} = 1.081151 \text{ \AA}$  have been optimized with the constraint of  $D_{2h}$  geometry via the B3LYP/6-311++G\*\* procedure of the GAUSSIAN code.<sup>20</sup>

The estimates arrived at via the DZ2 and PZ2 procedures<sup>13</sup> are very close to one another. The near-Hartree–Fock DZ2 results are partitioned in contributions from  $\sigma$  + core electrons and from  $\pi$ -electrons in Table 1.

(17) Since the induced magnetic field and the shielding density change sign on crossing the current flow, the net effect on a nearby probe depends on the radius  $r_{\text{L}}$  of the loop and the distance  $r_{\text{P}}$  of the probe from the loop center. If the ratio  $r_{\text{L}}/r_{\text{P}}$  is very small, the total field induced on the probe nearly vanishes. If this ratio is sufficiently large, canceling of shielding and deshielding contributions from the currents at A and B does not occur, and the sign of the field induced at  $r_{\text{P}}$  is mainly biased by the current nearest to the probe.

(18) Sauer, S. P. A.; Paidarova, I.; Oddershede, J. *Theor. Chem. Acc.* **1994**, *88*, 351.

(19) Diercksen, G.; McWeeny, R. *J. Chem. Phys.* **1966**, *44*, 3554.

**Table 1.** Orbital Contributions to Magnetic Susceptibility (in cgs ppm au) and Nuclear Magnetic Shielding (in ppm) of Cyclobutadiene<sup>a</sup>

property	xx	yy	zz	avg
$\chi$				
$\sigma + \text{core}$	-26.65	-156.69	-268.24	-150.55
$\pi$	-252.13	-86.40	226.85	-37.23
total	-278.78	-243.09	-41.39	-187.78
$\sigma_{\text{H1}}$				
$\sigma + \text{core}$	20.13	25.34	25.27	23.58
$\pi$	0.904	3.26	2.54	2.23
total	21.034	28.60	27.81	25.81
$\sigma_{\text{C1}}$				
$\sigma + \text{core}$	-45.08	101.98	130.24	62.38
$\pi$	-62.94	4.11	-7.18	-22.00
total	-108.02	106.09	123.06	40.38

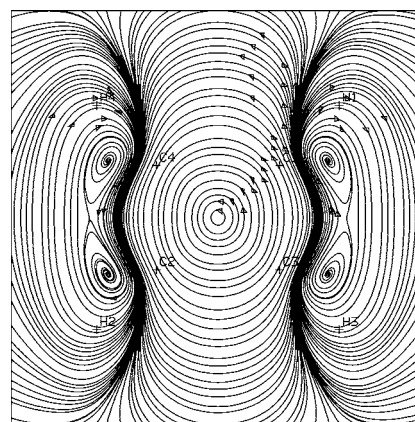
<sup>a</sup> CTOCD-DZ2 results from the (13s10p5d2f/8s4p1d) basis set for the  $D_{2h}$  constrained geometry. The conversion factor for susceptibility from cgs au per molecule to cgs emu per mole is  $a_0^3 N_A = 8.9238878 \times 10^{-2}$ ; further conversion to SI units is obtained by  $1 = \text{J T}^{-2} = 0.1 \text{ cgs emu}$ .

Figure 2 shows that a magnetic field perpendicular to the molecular plane of cyclobutadiene induces intense paramagnetic  $\pi$  flow in a sizable region about the  $C_2$  symmetry axis, encompassing the carbon skeleton and extending beyond the C–C single bonds. Diamagnetic  $\pi$  currents are observed in the regions of the CH bonds, on the side of each C=C bond, where the phase portrait of four foci,<sup>13</sup> i.e., streamlines spiralling along the  $z$  direction, is recognized. The paramagnetic  $\pi$  flow over the carbon double bonds is much stronger than that over the carbon single bonds. Therefore, the  $\pi$  ring current of cyclobutadiene can be ideally represented by a loop lying inside the carbon skeleton, as in the model of Figure 3.

The simple RCM of Figure 3 can be used to predict the essentials of the shielding density map for the H nucleus. Elemental shielding (deshielding) contribution at the site of the proton is expected from the  $\pi$  electron flow in the basin of the closest (furthest) carbon atom.

The ab initio maps for the  $\pi$  contribution to  $\Sigma_{zz}^{\text{H}}$  on the upper part of Figure 4 show a shielding spike-up in the vicinity of the *ipso* carbon and an elongated depression about the C=C bond on the opposite side, where the  $\pi$  ring currents cause deshielding at H, in full agreement with the model of Figure 3. Two more peaks, and a spike-down, are observed in the all-electron map on bottom of the figure, partially merging with those originating from  $\pi$  flow. The nodal region of  $\Sigma_{zz}^{\text{H}}$  lies close to the diagonal through C3 and C4. The

(20) Frisch, M. J.; Trucks, G. W.; Schlegel, H. B.; Scuseria, G. E.; Robb, M. A.; Cheeseman, J. R.; Zakrzewski, V. G.; Montgomery, J. A., Jr.; Stratmann, R. E.; Burant, J. C.; Dapprich, S.; Millam, J. M.; Daniels, A. D.; Kudin, K. N.; Strain, M. C.; Farkas, O.; Tomasi, J.; Barone, V.; Cossi, M.; Cammi, R.; Mennucci, B.; Pomelli, C.; Adamo, C.; Clifford, S.; Ochterski, J.; Petersson, G. A.; Ayala, P. Y.; Cui, Q.; Morokuma, K.; Malick, D. K.; Rabuck, A. D.; Raghavachari, K.; Foresman, J. B.; Cioslowski, J.; Ortiz, J. V.; Stefanov, B. B.; Liu, G.; Liashenko, A.; Piskorz, P.; Komaromi, I.; Gomperts, R.; Martin, R. L.; Fox, D. J.; Keith, T.; Al-Laham, M. A.; Peng, C. Y.; Nanayakkara, A.; Gonzalez, C.; Challacombe, M.; Gill, P. M. W.; Johnson, B. G.; Chen, W.; Wong, M. W.; Andres, J. L.; Head-Gordon, M.; Replogle, E. S.; Pople, J. A. *Gaussian 98*, revision A.7; Gaussian, Inc.: Pittsburgh, PA, 1998.



**Figure 2.** Ab initio ring-current model for cyclobutadiene. The plots display a view at points in a plane parallel to that of the molecule, displaced from it by 0.75 bohr, close to the maximum  $\pi$  electron density. Paramagnetic circulation is anticlockwise.

interpretation of the maps in Figure 5 is also eased by the model of Figure 3. However, it is expedient to compare the pattern in the upper part of Figure 5 with that observed in benzene. Since the most intense  $\pi$  ring currents in  $C_6H_6$  flow above the carbon nuclei (where maxima of the modulus  $|\mathbf{J}^{\text{B}}|$  are found), the node of the  $\Sigma_{zz}^{\text{C}}$  function approximately coincides with the position of the reference C nucleus. The outer (shielding) spike-up and the inner (deshielding) spike-down have similar size and their effects essentially cancel each other out. Therefore the net field induced at the C nucleus by the closest portion of the loop vanishes.<sup>21</sup>

The furthest segment of the  $\pi$  stream in the proximity of the para carbon provides a weak shielding contribution to the reference C nucleus, as expected from the model in Figure 1. The global effect of the  $\pi$  ring currents is that of shielding the reference C nucleus. This is confirmed by the calculated  $\pi$  contribution to  $\sigma_{zz}^{\text{C}}$ ,  $\sim +19 \text{ ppm}$ .<sup>13</sup>

The inverted pattern is observed for cyclobutadiene, with some significant differences.

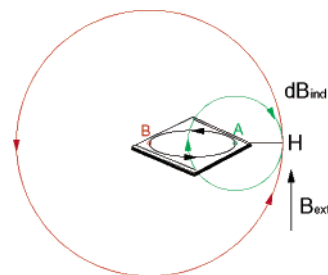


**Figure 3.** Ring-current model for cyclobutadiene from the DBS law. The external magnetic field  $\mathbf{B}_{\text{ext}}$  perpendicular to the molecular  $xy$  plane induces a paramagnetic (anticlockwise) current density in the  $\pi$  electrons. The  $\pi$  current through point A (B) generates an elemental magnetic field  $d\mathbf{B}_{\text{ind}}$ , green (red), diminishing (reinforcing)  $\mathbf{B}_{\text{ext}}$  at the site of the H proton, and causes shielding (deshielding) by enhancing (lowering) the out-of-plane component  $\sigma_{zz}^{\text{H}}$ .

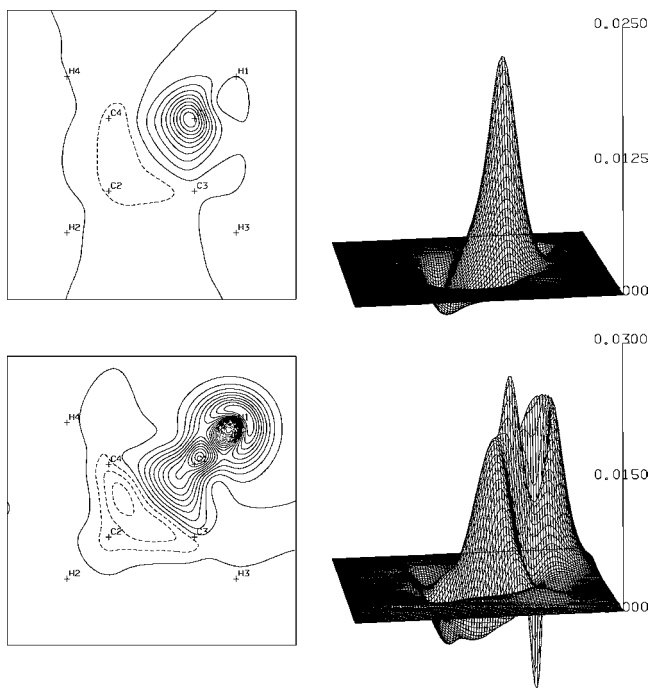


**Figure 4.** Proton magnetic shielding density  $\Sigma_{zz}^H$  on a plot plane displaced by 0.75 bohr from that of the cyclobutadiene molecule. In the contour map on the left, solid (dashed) lines mean positive (negative) values. For the  $\pi$  contribution, the values of the solid (dashed) lines decrease (increase) in steps of  $(2 \times 10^{-3})c^2$  au from the innermost contour at  $\sim(2 \times 10^{-2})c^2$  au (minimum at  $\sim(-4 \times 10^{-3})c^2$ ). In the all-electron map, the values of the solid (dashed) lines decrease (increase) by the same step from the innermost contour at  $\sim 0.023c^2$  au (minimum at  $\sim -0.015c^2$  au).  $c$  is the velocity of light,  $\sim 137.036$  au.

In this system, the paramagnetic  $\pi$  ring currents have maximum intensity all over a circuit internal to the carbon frame, so that the nodal line of the  $\Sigma_{zz}^{C1}$  of the reference C1 is slightly displaced inward. Therefore, the amplitude of the outer (deshielding) spike-down over the C1 nucleus, see Figure 5, is much smaller than that of the inner (shielding) spike-up, and cancellation between them does not occur. Apparently the shielding effect is stronger, but it is confined to a smaller area, compare the height of the spike-up with the depth of the spike-down nearby and the wide extension of the hollow region all around.

Deshielding caused by the current flowing in the other side of the loop is evidenced by the ditch in the zone of C2 and C4 (additional weak deshielding provided by the  $\sigma$  electron flow is observed in the maps on the lower part of Figure 5). The global effect of the paramagnetic  $\pi$  ring currents on the carbon nuclei of cyclobutadiene turns out to

(21) An observer, at the site of a reference C nucleus embedded in the diamagnetic  $\pi$  stream, looking in the direction of  $\mathbf{J}^B$ , and probing the effect of the streamline D on his right (L on his left), at a distance  $r_D(r_L)$ , experiences an induced flux density  $d\mathbf{B}_D \propto \mathbf{J}^B \times \mathbf{r}_D/|\mathbf{r}_D|^3 d^3r$  ( $d\mathbf{B}_L \propto \mathbf{J}^B \times \mathbf{r}_L/|\mathbf{r}_L|^3 d^3r$ ) parallel (antiparallel) to  $\mathbf{B}_{ext}$ . The streamlines D and L are assumed to be so close to one another that  $\mathbf{J}^B$  at  $r_D$  and  $r_L$  is the same. The opposite elemental fields cancel, and then no local ring current effect is expected the out-of-plane component  $\sigma_{||}^{C,12,13}$

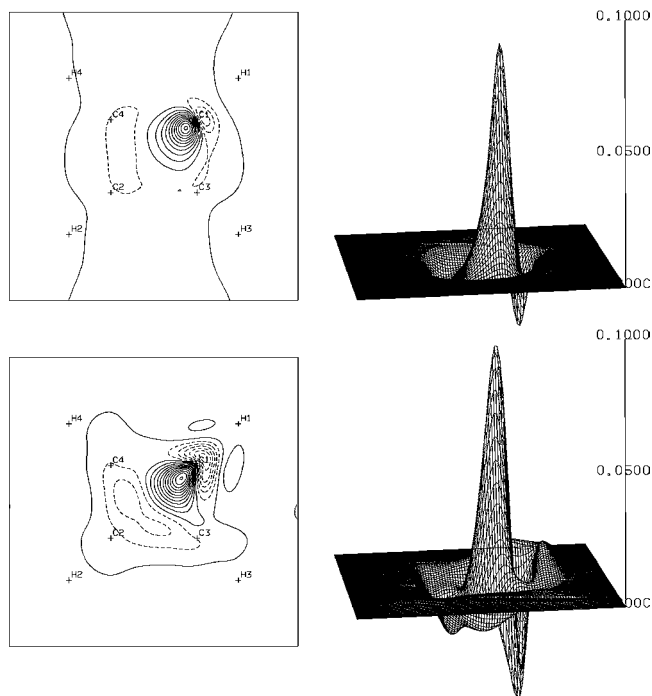


**Figure 5.** Carbon magnetic shielding density  $\Sigma_{zz}^C$  on a plot plane displaced by 0.75 bohr from that of the cyclobutadiene molecule. In the contour map on the left, solid (dashed) lines mean positive (negative) values. For the  $\pi$  contribution, the values of the solid (dashed) lines decrease (increase) in steps of  $(5 \times 10^{-3})c^2$  au from the innermost contour at  $\sim 0.08c^2$  au (minimum at  $\sim -0.03c^2$ ). In the all-electron map, the values of the solid (dashed) lines decrease (increase) by the same step from the innermost contour at  $\sim 0.09c^2$  au (minimum at  $\sim -0.05c^2$  au).

be deshielding, as shown in Table 1. The  $\pi$ -electron contribution to the out-of-plane component of carbon shielding is  $-7.2$  ppm.

The partitioning of the out-of-plane component of proton shielding in this Table confirms the predictions of the model: the positive  $\pi$ -electron contribution is  $\approx 2.5$  ppm. The  $\pi$  contribution to the out-of-plane component of the magnetizability of cyclobutadiene is also positive. The total  $\chi_{zz}$  is therefore approximately six times smaller in magnitude than the average in-plane component  $1/2(\chi_{xx} + \chi_{yy})$ . The consistence of different theoretical predictions provides further evidence for the validity of the model of Figure 3.

**Acknowledgment.** Financial support to the present research from the European research and training network NANOQUANT, and from the Italian MIUR (Ministero dell'Università e della Ricerca Scientifica e Tecnologica), via FIRB and 60% funds, is gratefully acknowledged.

**Note Added after ASAP Posting.** The author names in ref 6 were omitted in the version posted ASAP October 26, 2004; the corrected version was posted October 27, 2004.

OL048332M